LMA fibers based on two-dimensional solid-core photonic bandgap fiber design

Sergey L. Semjonov[*a], Olga N. Egorova[a], Alexey F. Kosolapov[a], Andrey E. Levchenko[a], Vladimir V. Velmiskin[a], Andrey D. Pryamikov[a], Mikhail Y. Salganskiy[b], Vladimir F. Khopin[b], Mikhail V. Yashkov[b], Alexey N. Guryanov[b], Evgeniy M. Dianov[a]
[a]Fiber Optics Research Center, 38 Vavilov Street, Moscow 199333, Russia;
[b]Institute of Chemistry of High-Purity Substances, 49 Tropinin Street, Nizhnii Novgorod 603950, Russia

ABSTRACT

Prospects of fabrication of solid-core photonic bandgap fibers with a large mode area (LMA) are discussed. Properties of solid-core photonic bandgap fibers with a small ratio of the cladding element diameter d to the distance Λ between neighboring cladding elements are studied. The range of fiber parameters at which the fiber is single-mode over the fundamental band gap is found.

Keywords: LMA fibers, microstructured fibers, solid-core photonic bandgap fibers.

1. INTRODUCTION

Recent progress in the development of fiber lasers and amplifiers generates a need for overcoming undesirable nonlinear effects appearing when laser radiation propagates in the fiber core. The threshold of nonlinear effects can be increased by decreasing the laser radiation intensity. For this purpose, fibers with a large mode field diameter can be used as the laser or amplifier media. Having a large mode diameter, these fibers should be simultaneously single-mode or nearly single-mode to ensure the high beam quality. One of the most successful approaches in manufacturing such fibers is the holey fiber design[1].

As demonstrated in [2], the large mode area together with single-modeness can be also obtained in solid-core photonic bandgap fibers. Typical cross sections of this type of fibers are shown in Fig. 1. The periodic fiber cladding is a two-dimensional photonic crystal. It is formed by cylindrical elements from germanium dioxide doped silica which are arranged in pure silica in the hexagonal order. The refractive index of germanium dioxide doped silica is higher than that of silica, the refractive index contrast in the cladding being about 1-2%. The fiber core formed by omitting one or more elements confines light within band gaps of the photonic crystal.

The all-solid bandgap fiber was first demonstrated in [3]. In that paper and in a number of later publications, the ratio of the cladding element diameter d to the distance between neighboring elements Λ (Fig. 1) exceeded 0.34. In [2] it was shown for the first time that all-solid bandgap fibers can also localize light and have a relatively low optical loss (20 dB/km) at a small ratio of the cladding element diameter to the distance between neighboring elements (d/Λ=0.12). At the same time it can have a large mode field diameter and be single-mode in a wide spectral range. This fact provides enough reasons to investigate prospects of using such fibers as an active media of lasers and amplifiers. An important advantage of all-solid bandgap fibers is the absence of air holes in the fiber cross section, which makes fabrication and handling of these fibers easier compared to holey microstructured fibers [1].

It is also worth noting that at small values of d/Λ, such fibers can be clad-pumped through the fiber end. Because cladding elements are waveguides, the part of the pump power will be captured by them upon the end cladding pumping. At small ratio of the cladding element diameter to the distance between elements (d/Λ<0.2), the captured part of pump radiation will be negligible (a few per cent) in contrast to large d/Λ.

[*] sls@fo.gpi.ru

Fiber Lasers VII: Technology, Systems, and Applications, edited by Kanishka Tankala, Jay W. Dawson,
Proc. of SPIE Vol. 7580, 758018 · © 2010 SPIE · CCC code: 0277-786X/10/$18 · doi: 10.1117/12.841265

In this paper, we analyze how properties of the all-solid photonic bandgap fiber with a small value of d/Λ depend on cladding and core parameters. This issue is important in connection with possible application of these fibers as laser and amplifier media. The range of fiber parameters at which the fiber is single-mode over the fundamental band gap is found.

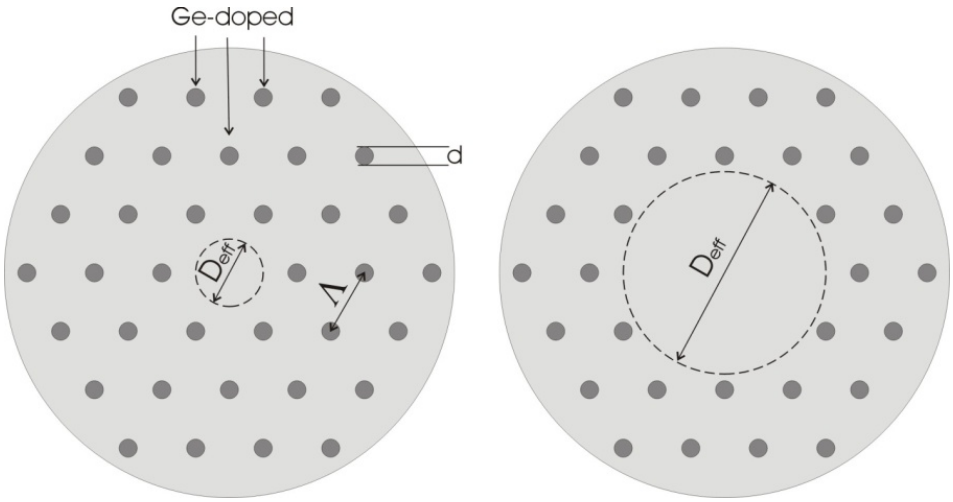

Figure 1. Fiber cross section with a core formed by one and seven omitted cladding elements.

2. NUMERICAL MODELING

To determine how the band gaps and mode structure of the fiber core depend on the fiber parameters, we calculated numerically the band diagram and dispersion curves of the core modes at different core and cladding parameters. The band structure and dispersion curves of the core modes were calculated by the plane-wave method[4] using the MIT Photonic-Bands (MPB) software[5]. Band structures were computed using a simple cell, while the dispersion curves of the core modes were computed using a super cell $6\Lambda X6\Lambda$. We also calculated the core modes by the multipol method, using the software package CUDOS MOF[6]. The difference between effective refractive indices obtained with plane-wave and multipol methods only insignificantly alters the dispersion curves; the mode structure was always the same. The calculation was made for three refractive index contrasts in the cladding Δn: 0.005; 0.015 and 0.03. For each refractive index contrast value, the calculation was preformed for five ratios of the cladding element diameter to the distance between neighboring elements d/Λ: 0.05, 0.1, 0.2, 0.3, 0.4. The core was formed by omitting one or seven elements. For all combinations of the cladding and core parameters, the band diagrams and dispersion curves of the core modes were calculated.

The band diagram of the solid-core photonic bandgap fiber with d/Λ=0.1 and refractive index contrast Δn=0.015 in the cladding is shown in Figs. 2a, b. The band structure is mapped as a function of λ/Λ and $(\beta-kn_0)\Lambda$, where λ is the wavelength, β is the mode propagation constant, $k=2\beta/\lambda$, n_0 is the refractive index of silica. The allowed bands of the photonic crystal are shown in grey. These regions depend only on the parameters of the periodic cladding and do not depend on the core design. The band gaps are shown in white. Three band gaps of the photonic crystal cladding are shown in Figs. 2a, b, but we investigate only the band gap 'I' (the fundamental band gap). The band structure for other cladding parameters looks similar.

The dispersion curves of core modes in these figures are shown in black. Core lines lie in the band gap below the silica line $-(\beta-kn_0)\Lambda=0$. In the region denoted '1-2' in Fig. 2a the dispersion curves of the core mode can exist between the silica line and lower band gap edge β_L, in the region '2-3' − between upper and lower band gap edges β_U, β_L. Each mode has a short-wavelength cutoff at the point *a* where the dispersion curve crosses the lower band gap edge, and a long-wavelength cutoff at the point *b* where the dispersion curve crosses the upper band gap edge.

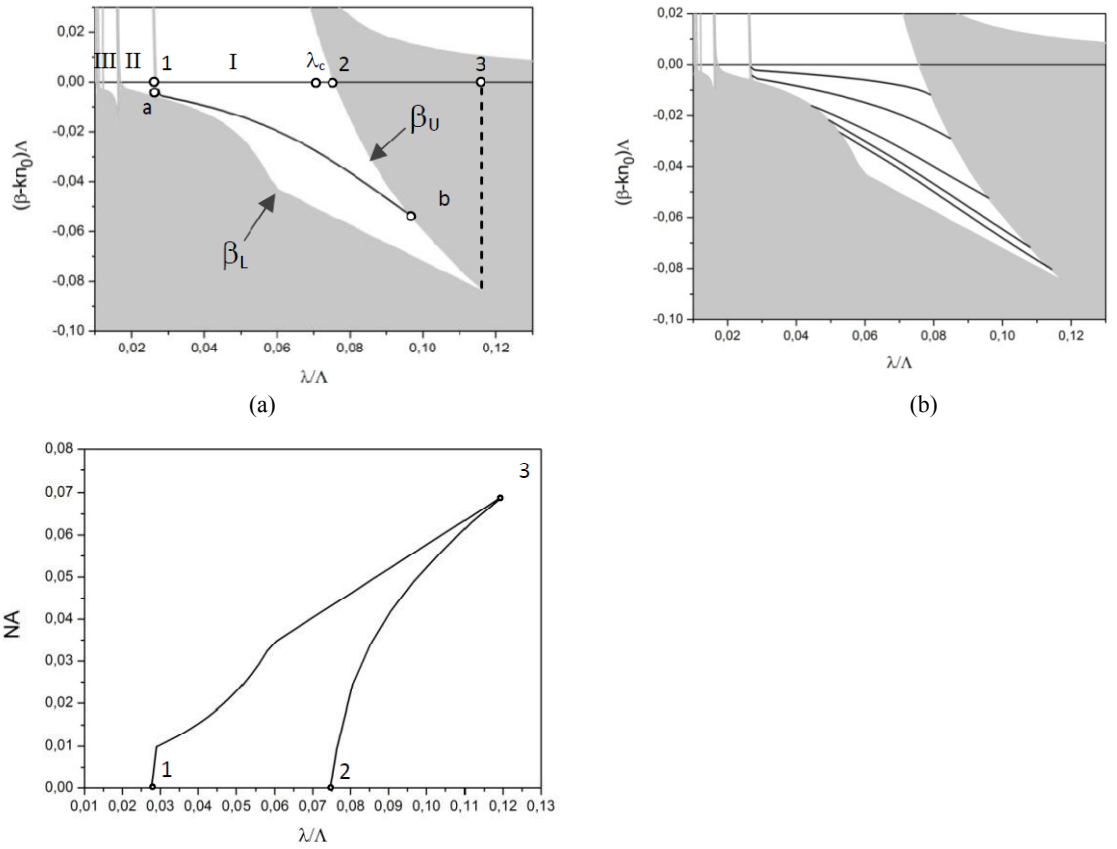

Figure 2. Band diagrams of the fiber with the refractive index contrast Δn=0.015 in the cladding and the ratio of the cladding element diameter to the distance between neighboring elements d/Λ=0.1, and the core formed by omission of one (a) and seven (b) elements. (c) is the equivalent *NA* of the fiber.

The calculated band gap edges β_L and β_U for different cladding parameters are plotted versus λ/Λ in Fig. 3. It is shown how the band gap changes at different refractive index contrast in the cladding Δn (d/Λ is fixed) Fig. 3(a) and how it changes at different d/Λ (Δn is fixed) Fig. 3(b). If values of d/Λ and Δn decrease, the fundamental band gap shifts to smaller λ/Λ and becomes shallow.

Two parameters can be introduced to characterize the band gap: the relative bandwidth and the band gap depth. The relative bandwidth $\Delta\lambda$ is equal to $(\lambda_3-\lambda_1)/\lambda_c$, where λ_3 and λ_1 are highest and lowest band gap wavelengths at points 1 and 3 (Fig. 2a); $\lambda_c=(\lambda_3+\lambda_1)/2$ is the central wavelength of the band gap. Note that the relative bandwidth characterizes only the band gap. The guided core mode exists in the range where its dispersion curve lies within the band gap (a−b in Fig. 2a). The spectral range, where the core mode exists, is narrower than the spectral width of the band gap and depends on the core design.

The effective refractive index $n_{eff}=\beta/k$ at the central wavelength of the band gap λ_c can be used as the band gap depth.

The Figure 4 shows the relative bandwidth and $n_{eff}(\lambda_c)-n_0$ as functions of d/Λ for different Δn (0.005, 0.015 and 0.03). The relative bandwidth is almost independent of d/Λ and Δn. Conversely, the effective refractive index $n_{eff}(\lambda_c)$ at the central wavelength of the band gap λ_c is strongly affected by a change in the cladding parameters and decreases with increasing d/Λ and Δn.

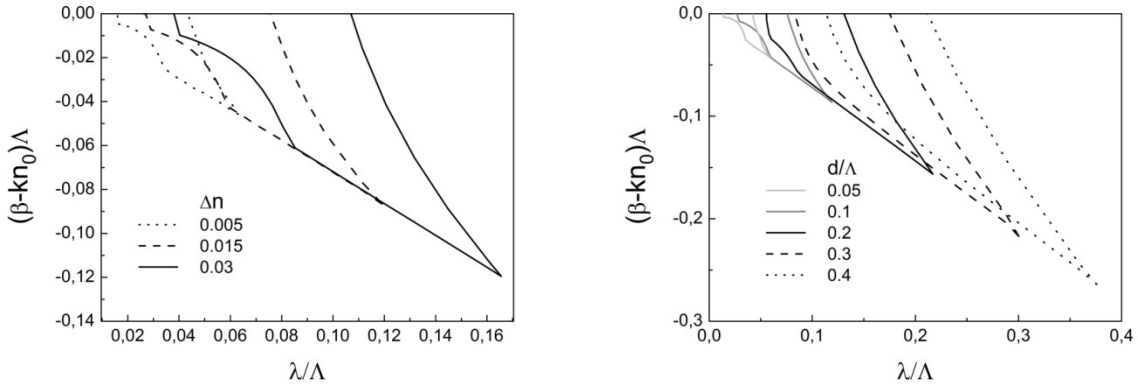

(a) (b)

Figure 3. Calculated band gap edges β_L and β_U for different cladding parameters versus λ/Λ: (a) d/Λ=0.1, (b) Δn=0.015.

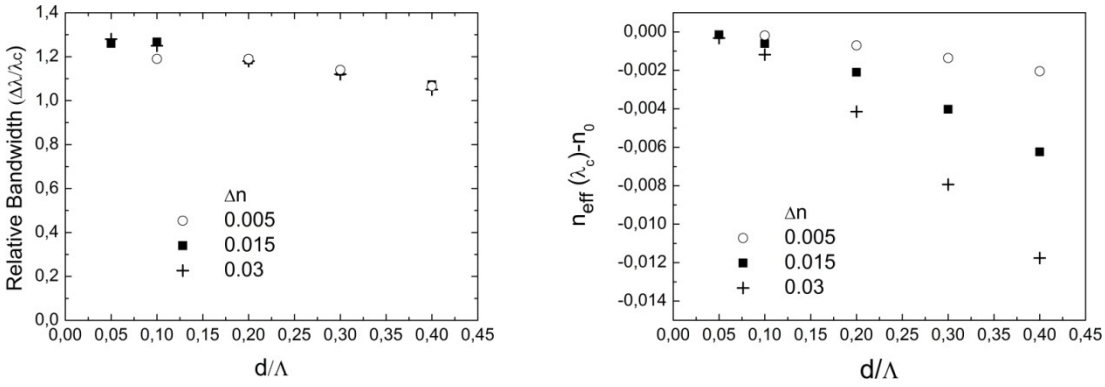

(a) (b)

Figure 4. Relative bandwidth and difference between effective refractive index of the center of the band gap and refractive index of silica versus d/Λ for different values of the refractive index contrast in the cladding.

To determine how the mode structure of the fiber core depends on fiber parameters we calculated numerically the dispersion curves of the core modes of the all-solid bandgap fiber at different core and cladding parameters (Fig. 2a,b). The calculation shows that if only one element is omitted to form the core, there is only one core mode all over the fundamental band gap (Fig. 2a). This is the fundamental core mode HE11, doubly degenerated because of two polarization states. The result is the same for all combinations of the cladding parameters. So the fiber is single mode at any fiber cladding parameters in the investigated range, when one element is omitted to form the core.

In the case of the seven-element core, there are 14 core modes within the fundamental band gap (Fig. 2b). As some of them are degenerated, they form five groups with nearly identical dispersion curves. This mode structure is similar to that of solid-core holey-cladding fibers[7]. The results of calculations for other cladding parameters look similar and have the same mode structure.

3. EXPERIMENTAL RESULTS

We fabricated fibers with one and seven omitted cladding elements. Fiber parameters are listed in Table 1. Fiber end-faces are shown in Fig. 5. Fibers have been manufactured by the stack and draw technique. The elements for the cladding were drawn from MCVD performs doped with germanium dioxide.

Table 1. Parameters of fabricated fibers.

	d/Λ	Λ, μm	Δn	Number of elements omitted to form the core	Number of cladding layers	Mode structure
1	0.24	9.2	0.0185	7	6	Multimode
2	0.08	18	0.028	7	2	Multimode
3	0.12	11.4	0.028	1	6	Single-mode
4	0.09	28.8	0.005	1	3	Single-mode

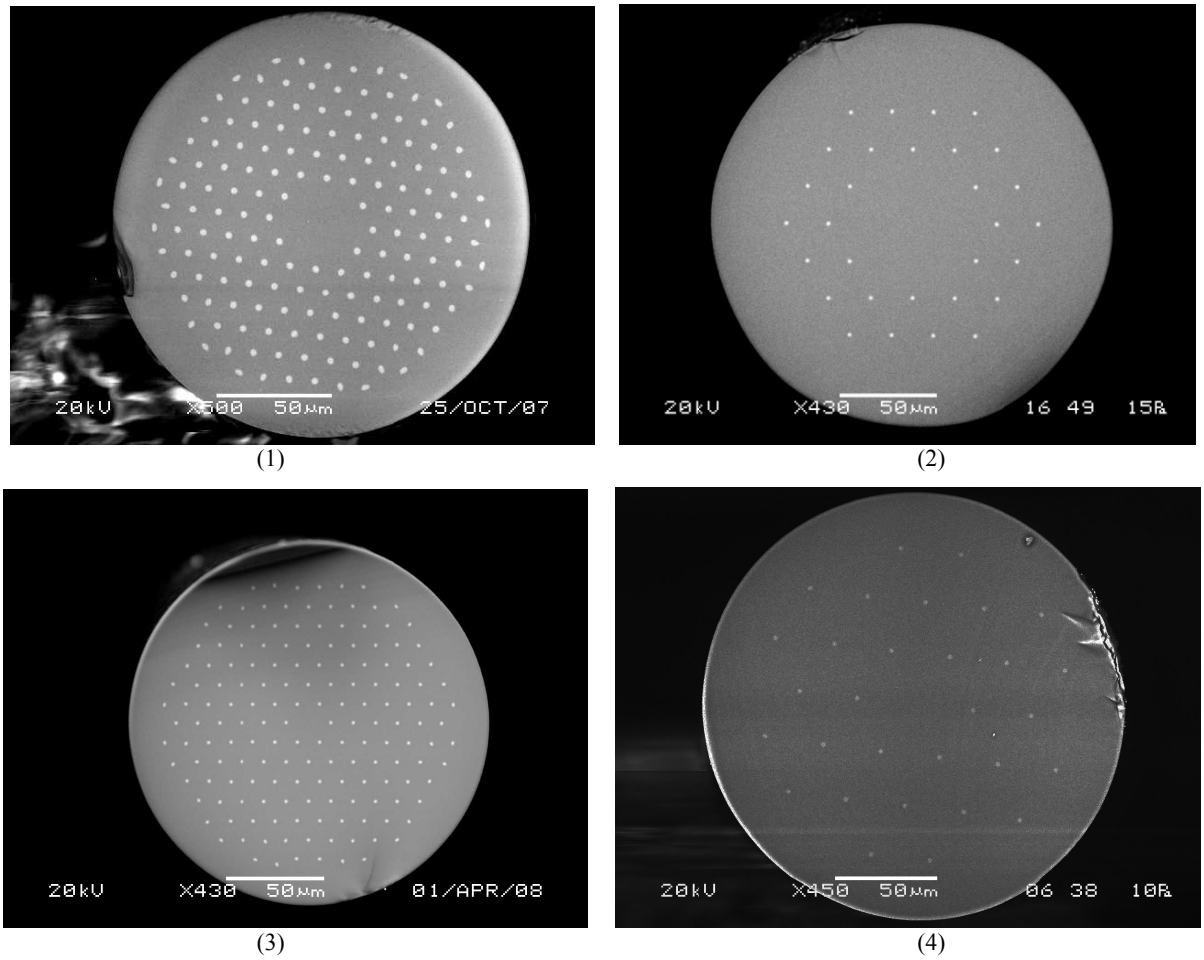

(1) (2)

(3) (4)

Figure 5. Scanning electron micrographs of end-faces of fiber samples listed in Table 1. White spots are high-index Ge-doped regions.

We investigate the mode structure by examining the near-field pattern of the core mode using an external light source at different launching conditions. The experimental observations confirm that fibers with one-element core are single-mode, with seven – multi-mode.

To make a single-mode fiber (with the core formed by omitting only one element) with a large core diameter, we increased the distance Λ between neighboring elements to 28.8 μm (sample 4 from Table 1). As it follows from Fig. 3, when λ is fixed, and Λ increases (λ/Λ decreases), the fundamental band gap exists at smaller refractive index contrasts in the cladding (Δn) and smaller ratios of the cladding element diameter to the distance between neighboring elements (d/Λ). So fiber 4 was fabricated with small d/Λ= 0.09 and Δn=0.005. As shown in Figure 4a, a relatively wide spectral range can be achieved even for such small values of this parameters. SEM of fiber end-face is shown in Fig. 5. The outer diameter of the fiber was 200 μm. As the distance between cladding elements is very large, only three cladding layers can be put within this outer diameter.

Figure 6a shows the band diagram of fiber 4. The dispersion curve of the core mode intersects the band gap edges at 0.4 and 1.4 μm. In the range of 0.4−0.7 μm, the dispersion curve is very close to the band gap edge.

The near-field pattern of the core mode was observed with a CCD-camera in the range of 0.8−1.15 μm (Fig. 6b). The long-wavelength edge of this region was limited by the CCD-camera. At different launching conditions, the near-field pattern remains Gaussian with mode field diameter 34 μm at 1.05 μm.

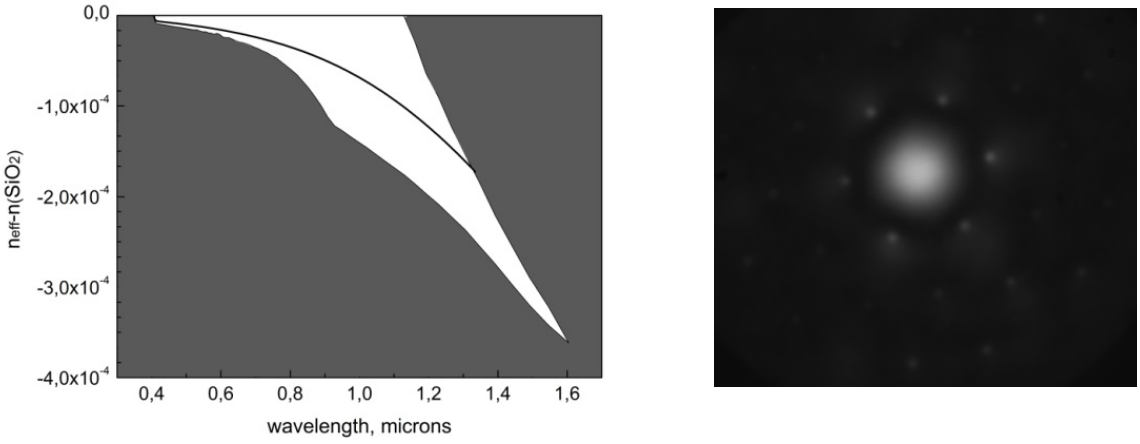

(a) (b)

Figure 6. Band diagram for Fiber 4 (a). Y axis is n_{eff}-n(SiO_2), where n(SiO_2) is the refractive index of silica. Near field pattern at a wavelength of 1.05 μm (b).

The transmission spectra were measured using a 2-m-long straight fiber. The transmitted light was observed with a photo detector in the spectral range of 0.8—1.3 μm. This range closely coincide with the results of theoretical modeling (Fig. 6a). Optical losses were measured by the cut-back technique in a straight fiber. The measured loss was 6 dB/m at 1−1.2 μm.

So, by enlarging the distance between the neighboring elements with a one-element core, mode field diameter 34 μm along with single-modeness can be achieved in a relatively wide spectral range. However, a small number of cladding layers and small ratio of the cladding element diameter to the distance between neighboring elements results in unsuitable high losses in this specific fiber sample.

4. EQUIVALENT *V*-PARAMETER

The behavior of the all-solid bandgap fiber can be understood in terms of the equivalent fiber with a step-index profile. The analogy to conventional step-index fibers can be applied to the all-solid bandgap fiber in a similar way as it was done in [8] for the hollow-core bandgap fiber and in [9], [10] for solid-core holey-cladding fibers. The step-index fiber can be characterized by the *V*-parameter

$$V = \frac{2\pi R\sqrt{n_{co}^2 - n_{cl}^2}}{\lambda} = \frac{\pi DNA}{\lambda} \quad ,$$

where $D=2R$ is the fiber core diameter; n_{co}, n_{cl} are refractive indices of the core and of the cladding, respectively; *NA* is the numerical aperture. The *V*-parameter determines the number of modes [11] $N = \frac{V^2}{2}$.

The equivalent numerical aperture *NA* can be defined for the all-solid photonic bandgap fiber from the calculated band diagram (Fig. 2a). The mode with a propagation constant β propagates at the angle θ relative to the fiber axis, which is equal to $\theta = arccos\left(\frac{\beta}{kn_0}\right)$. The band gap edges define the maximum $\theta_{max} = arccos\left(\frac{\beta_L}{kn_0}\right)$ and minimum $\theta_{min} = arccos\left(\frac{\beta_U}{kn_0}\right)$ allowed propagation angles of the core modes. Thus the equivalent numerical aperture of the fiber core in region '1-2' is equal to $NA = n_0 \sin(\theta_{max}) = \sqrt{\mathrm{n}_0^2 - \left(\frac{\beta_L}{\mathrm{k}}\right)^2}$. In region '2-3' there are maximum and minimum numerical apertures: $NA_{min} = \sqrt{\mathrm{n}_0^2 - \left(\frac{\beta_U}{\mathrm{k}}\right)^2}$ and $NA_{max} = \sqrt{\mathrm{n}_0^2 - \left(\frac{\beta_L}{\mathrm{k}}\right)^2}$.

The spectral dependence of the *NA* of the solid-core photonic bandgap fiber can be computed using the band diagram (Fig. 2c). The acceptance angles of the fiber core correspond to the numerical aperture lying within curve 1-2-3. The equivalent *NA* is the function of periodic cladding parameters and does not depend on the core design.

In contrast to the conventional step-index fiber, the core diameter cannot be exactly defined in the all-solid bandgap fiber. As the core diameter, we will use some effective value $D_{eff}=\eta\Lambda$, where η is some coefficient (Fig. 1). The unknown coefficient η does not greatly depend on the wavelength and cladding parameters, but basically depends on the number of cladding elements which were omitted to form the core (as in Fig. 1).

Therefore, the equivalent normalized frequency of the solid-core photonic bandgap fiber is:

$$V = \frac{\pi D_{eff} NA}{\lambda} = \frac{\pi\,\eta\,\Lambda\,NA}{\lambda}.$$

To investigate the influence of fiber cladding parameters on the mode structure, it is worthwhile to use the parameter V/η, which does not depend on the core design. Using the band diagrams calculated in the previous section, we can find V/η. Figure 7 shows the calculated V/η plotted against λ/Λ for different cladding parameters. Calculations were performed for refractive index contrasts in the cladding (Δn = 0.005, 0.015 and 0.03), as well as for the ratio of the cladding element diameter to the distance between neighboring elements (d/Λ = 0.05, 0.1, 0.2, 0.3, 0.4). One can see from Fig. 7, that the parameter V/η reaches a maximum value and does not vary significantly in the major part of the band gap. The maximum value of V/η is approximately 1.6−1.8.

Assuming that the coefficient η does not greatly depend on the cladding parameters and wavelength, it follows that the *V*-parameter also reaches nearly constant maximum value $V=1.8\eta$, the same for all curves, and does not vary significantly within the fundamental band gap. Because the *V*-parameter determines the mode number of the fiber, the maximum mode number should be nearly the same in all fibers with the same core design. Thus the maximum number of core modes in the fundamental band gap of the solid-core photonic bandgap fiber in the investigated range of cladding parameters is not greatly affected by refractive index contrasts in the cladding and by the ratio of the cladding element diameter to the distance between neighboring elements, but substantially depends on the numbers of elements omitted to form the core.

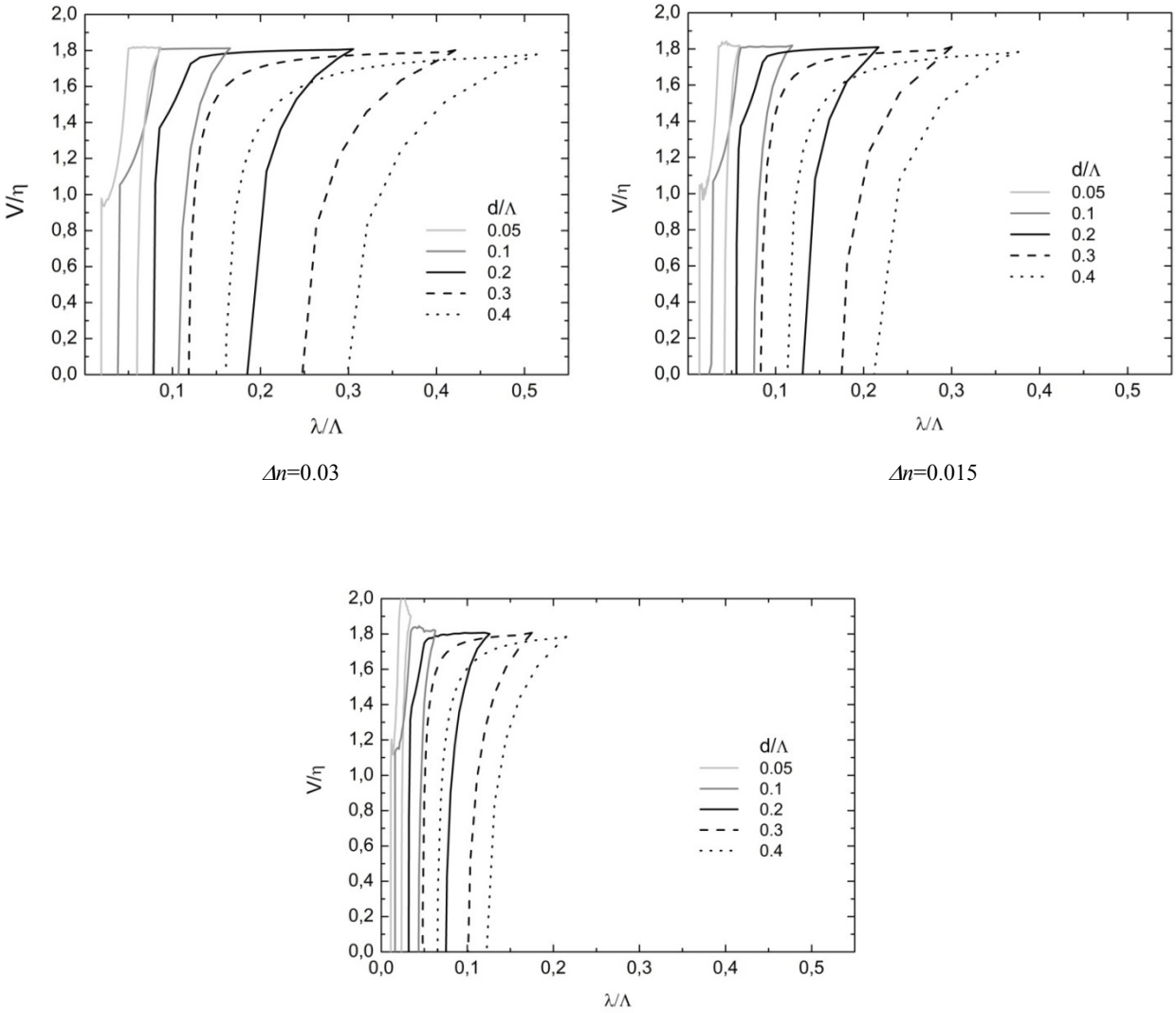

Figure 7. Calculated parameter V/η for different refractive index contrasts in fiber cladding. At each plot, five curves correspond to different d/Λ.

5. CONCLUSION

We showed how the fiber cladding and core design influence on the mode structure of the all-solid bandgap fiber. We investigated fibers with a small ratio of the cladding elements diameter to the distance between neighboring elements ($d/\Lambda \leq 0.4$) and the refractive index contrast Δn in the range of 0.005−0.03. Because the solid-core bandgap fiber with small d/Λ can have a large mode field diameter and be single-mode in a wide spectral range, this study is interesting in connection with possible applications of these fibers as laser and amplifier media.

Both calculations and experiments showed that the mode structure depends only on the core design and is not affected by the cladding parameters in the range under study. If the core is formed by omission of one cladding element, the fiber is always single-mode, if by seven omitted elements, it is a multimode one.

REFERENCES

[1] Knight, J C; Birks, T A; Russell, P St J; Atkin, D M, "All-silica single-mode optical fiber with photonic crystal cladding, " Optics Letters 21(19), 1547-1549 (1996).

[2] O.N. Egorova, S.L. Semjonov, A.F. Kosolapov, A.N. Denisov, A.D. Pryamikov, D.A. Gaponov, A.S. Biriukov, E.M. Dianov, M.Y. Salganskii, V.F. Khopin, M.V. Yashkov, A.N. Gurianov, D.V. Kuksenkov , "Single-mode all-silica photonic bandgap fiber with MFD 20 μm," Opt. Express 16, 11735-11740 (2008).

[3] A. Argyros, T. A. Birks, S. G. Leon-Saval, C. M. B. Cordeiro, F. Luan, P. St.J. Russell, "Photonic bandgap with an index step of one percent," Opt. Express 13, 309-14 (2005).

[4] Steven G. Johnson and J. D. Joannopoulos, "Block-iterative frequency-domain methods for Maxwell's equations in a planewave basis," Opt. Express 8, 173-190 (2001).

[5] ab-initio.mit.edu/mpb.

[6] T.P. White, B.T. Kuhlmey, R.C. McPhedran, D. Maystre, G. Renversez, C. Martijn de Sterke, and L.C. Botten, "Multipol method for microstructured optical fibers. I. Formulation," J. Opt. Soc. Am. B 19, 2322-2330 (2002).
B.T. Kuhlmey, T.P. White, G. Renversez, D. Maystre, L.C. Botten, C. Martijn de Sterke, and R.C. McPhedran, "Multipol method for microstructured optical fibers. II. Implementation and resultes," J. Opt. Soc. Am. B 19, 2331-2340 (2002).

[7] R.Guobin, W.Zhi, L.Shuqin, J.Shuisheng, "Mode classificacation and degeneracy in photonic crystal fibers," Opt. Express 11, 1310 (2003).

[8] M.J.F.Digonnet, H.K.Kim, G.S.Kino, S.Fan, "Understanding Air-Core Photonic-Bandgap Fibers: Analogy to Conventional Fibers," J. of Lightwave Tech. 23, 4169-4177 (2005).

[9] T.A.Birks, J.C. Knight, and P.St.J. Russell, "Endlessly single mode photonic crystal fiber," Opt. Lett. 22, 961-963 (1997).

[10] N.A.Mortensen, J.R.Folkenberg, M.D.Nielsen, K.P.Hansen, "Modal cutoff and the V parameter in photonic crystal fibers," Opt. Lett. 28, 1879-1881 (2003).

[11] D.Gloge, "Weakly guiding fibers," Applied Optics 10, 2252-2258, (1971).